Nanosized Hydroxyapatite

Subjects: Materials Science, Biomaterials

Contributor: Juan Ruso

The development of new materials based on hydroxyapatite has undergone a great evolution in recent decades due to technological advances and development of computational techniques.

hydroxyapatite tissue engineering bones porous materials biomaterials regenerative medicine

1. Introduction

The history of mankind is closely related to technological development. Depending on the most characteristic resources or tools, we have spoken of the stone age, bronze, iron, wood, coal, steel, petrol, and semiconductors. Nowadays, the confluence of techniques and methods from disciplines such as physics, chemistry, biology or engineering has given rise to what is known as materials science and within this discipline, and much more recently, what are known as smart materials have emerged, i.e., materials designed and manipulated to adapt and respond in a controlled manner to specific stimuli [1].

Traditionally, the development of materials has been based on the use of many elements and resources. Today, for the design of smart materials, many scientists have been inspired by the elegant solutions offered by nature. Natural materials, or biomaterials, consist of a small number of building blocks, which are therefore lighter and more abundant, to design a huge variety of structures. The key lies in a hierarchical structure, i.e., different levels of organization from basic units at the lowest level to much more complex ones at higher levels. In this way, using relatively few building blocks, a great variety of minerals, macromolecules, cells, organs and even persons have been created [2][3]. In this sense, hydroxyapatite (HAP) is an example of unity and duality, a substance that is both a mineral and a biological material. From the mineral point of view, it belongs to the apatites group, with general formula Ca5(PO4)3X, where, depending on the element X, they are classified as fluoropatite (F), chloropatite (Cl) and hydroxyapatite (OH). They generally crystallize within the hexagonal rhombic prism with space group P63/m and unit cell dimensions: a = 9.432 Å and c = 6.881 Å. The presence of crystalline calcium phosphate is what determines that it can crystallize into hydroxyapatite and betawhitlokite salts depending on factors such as Ca/P ratio, hydration state, impurities, and temperature. The color of the crystals can be neutral or vary from red to brown, due to iron oxide. HAP has a density of 3.16 gcm^{-3}, a hardness of 5 Mohs, a melting point above 1500 °C and in nature it is found in sedimentary and metamorphic rocks. This mineral is one of the most exclusive minerals and therefore, it is not easy to find deposits anywhere in the world. From the biological point of view, hydroxyapatite and its precursors are present in different animal groups from corals or starfish to vertebrates, where it is the main

inorganic constituent of bone tissues and dental enamel [4][5][6]. In living beings, it does not act alone. To fulfill its function, it works together with collagen, which is a fibrous protein of the connective tissues.

It is common to show graphs with the evolution of the number of papers published in a particular area. This type of representation does not reflect the weight that this area represents within the major scientific disciplines. In fact, as Larsen and von Ins showed, the number of publications between 1907 and 2007 has grown in all disciplines, due to the increased number of publications in all disciplines due to several factors discussed in their paper [7]. For this reason, in Figure 1, we show the number of papers where hydroxyapatite and biomaterials were employed during the last 30 years. Representing both key words, the weight of papers focused on hydroxyapatite remains intact despite the boom that the area of biomaterials has experienced in the last years [8].

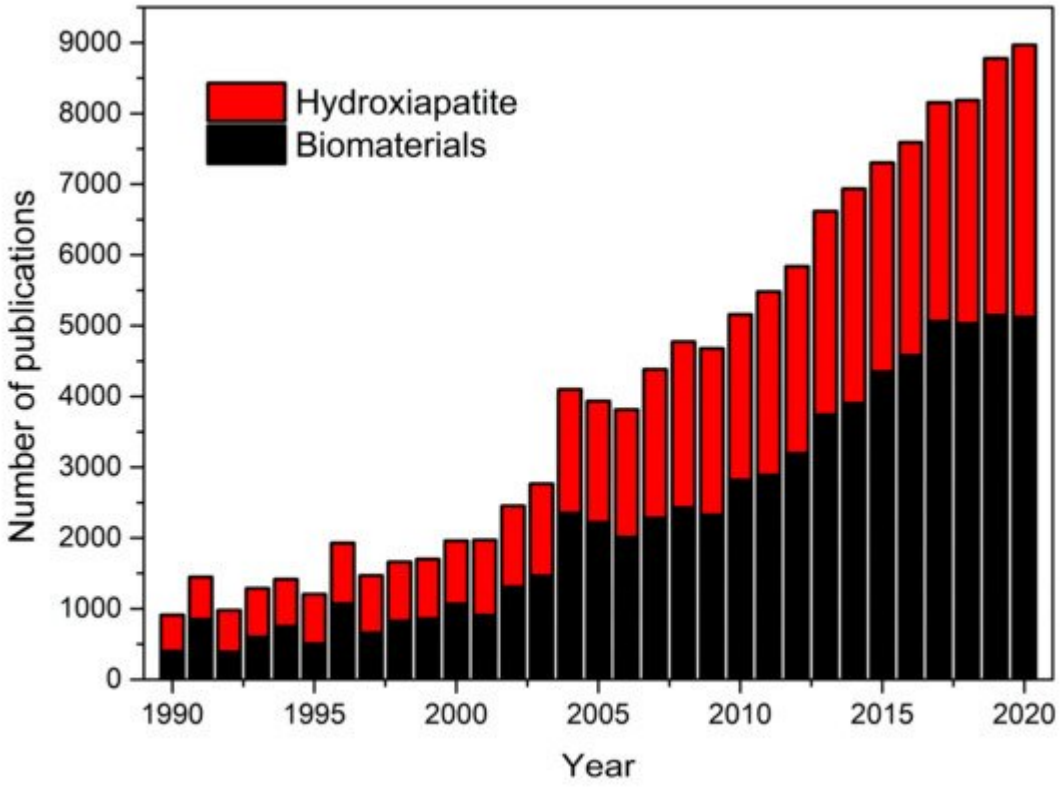

Figure 1. Scientific publications from 1990 to 2202 based on a Scopus database search performed in March 2021 on the topics “Biomaterials” and “Hydroxyapatite” (TITLE-ABS-KEY).

In the field of biomaterials, HAP is classified as a bioactive material; that is, when it interacts with biological entities it can form interfacial bonds that, more precisely, manifest as chemical bonds between hydroxyapatite and the adjacent biological tissue. In fact, medical trials have underscored the biocompatible, bioactive, biostable and osteoconductive capabilities of hydroxyapatite [9]. It is precisely these properties that have made it one of the most widely used materials not only in those areas of medicine related to hard tissues such as: traumatology, maxillofacial or dentistry [10][11], but also in orbital implants [12]. Within these areas there it can be found either as a monolith, coatings or as one of the components of composites [13]. On the other hand, several recent studies have shown the versatility of this material, either in its pure state or combined with other elements in areas completely

unrelated to tissue engineering such as: water purification, batteries, drug delivery, catalysis, ion exchange, and sensors [14][15].

Consequently, the aim of this review is to evaluate and offer a general overview about the current knowledge on hydroxyapatite based smart materials supplied by different approaches. In the compilation of this review an attempt has been made to give appropriate recognition to the current interest in most common and emergency applications, by discussing such aspects as newer systems, unusual approaches and highly used techniques including information about the physical principles and effectiveness of selected techniques (Scheme 1 depicts a flow diagram of the structure of this review). The development of nano-hydroxyapatite-based systems has raised certain misgivings; despite being chemically the same, their reduced dimensions mean that they can be easily absorbed by cells, creating adverse effects, such as cytotoxicity, induction of oxidative stress, apoptosis, and inflammatory responses. Therefore, part of this summary focuses on the evaluation of these systems. For this purpose, we have focused not only on the experimental point of view, but also in the computational one. The review is organized by techniques with the same format: beginning with a small introduction and a discussion of the specific approaches, applications and papers that are mainly based on it. It is almost impossible to cover all current techniques; therefore, we have chosen those more popular and accessible in most laboratories all over the world. Further, because of space limitations and the recent upsurge of interest in biotechnology and biomedical areas, the cited articles represent only a small fraction of the total number published in recent years.

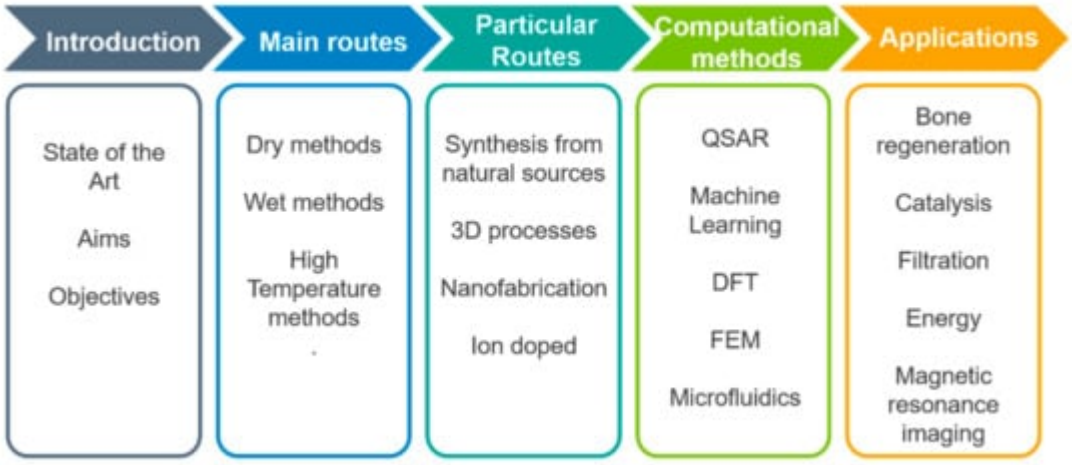

Scheme 1. Flowchart describing the structure of this review.

2. Main Routes of Hydroxyapatite Production

In the previous section we commented that there is natural hydroxyapatite that has two major drawbacks: the presence of impurities is very high and the morphology and texture, especially at the micro scale, are predetermined. In contrast to these compounds, synthetic HAP offers the advantage of both purity and the possibility of selecting different variables such as Ca/P ratio, porosity or hardness. Thus, the number of HAP synthesis routes is large due to the different applications and the versatility of the material. There is practically a

route for each specific design or application, so depending on the needs, the objectives can be to obtain HAP in powder, granular, macro- or microporous form, with different degrees of crystallinity and so on.

Although there are different classifications of synthesis routes, most authors advocate classifying them into three types: dry, wet, and high temperature processes [16][17][18][19][20][21][22]. Dry methods are sub classified in solid state and mechanochemical methods. In solid state methods, chemical precursors (such as Ca3(PO4)2 and CaCO3, CaP2O7 and CaCO3, or CaHPO4, 2H2O and CaO) are calcined, between 900 and 1300 °C, to obtain HAP. Basically, these processes involve the solid-state diffusion of ions from the precursors during calcination [23]. In mechanochemical processes, the chemical reaction of the precursors is induced by the action of mechanical processes such as milling or compression. The most common equipment is mixer mill and planetary mill. Rotation speed and milling time affect the obtained product: higher rotation speed increases crystallinity and crystallite size but reduces the particle size and the agglomeration of particles. On the other hand, milling time affects the HAP size and morphology. Generally speaking, dry processes ensure the formation of stoichiometric HA (Ca:P = 1.67) but require much power and time. Moreover, the products of such processes typically lack homogeneity [24][25].

The wet processes involve HAP precipitation by mixing aqueous solutions of compounds carrying Ca^{2+} and $PO4^{3-}$. It is the largest group, and the different routes are classified as low-temperature chemical precipitation, hydrolysis reaction and hydrothermal method [26][27][28][29][30]. The HAP obtained by the first method usually are porous and with inhomogeneous chemical composition. The last one provides well-crystallized powders with homogeneous chemical composition [31]. In this type of synthesis, factors such as morphology, crystallinity and chemical structure show an extreme dependence on the different synthesis parameters such as reactant addition rate, concentration, drying/heat treatment conditions, and, especially, pH and temperature. The order in which the reagents are added for mixing is very important. The calcium should be added slowly to the phosphorus, otherwise the formation of pure, crystalline hydroxyapatite is hindered. The residence time plays an important role in the synthesis of pure hydroxyapatite. For short resting times, dicalcium phosphate and undefined amorphous phases may appear in addition to hydroxyapatite [32]. Sintering temperature and atmosphere are also relevant, as these factors negatively affect the mechanical strength of HAP: high sintering temperatures cause the removal of OH groups in the HAP matrix, converting part of the HAP phase into α-tricalcium phosphate, β-tricalcium phosphate and tetracalcium phosphate. In addition, this decrease in HAP phase causes the densification to disappear, negatively affecting the mechanical properties [33]. The main advantages of these methods are that they are usually the simplest and most economical routes. On the other hand, the by-product is mostly water and the probability of contamination during synthesis is very low.

Due to the great impact that HAP has on materials intended for tissue regeneration, it is important to highlight the impact of the synthesis route and methodology on the viability and final functionality of the product [34]. In this sense, powders' strength and osteointegration are critical characteristics that depend significantly on their microstructure. Therefore, the main challenge in the synthesis of HAP for medical purposes is to control the morphological parameters that can affect its mechanical properties, biocompatibility and bioactivity [35]. In this field it is important to bear in mind that bone tissue is not uniform and has specific characteristics, for example compact or cortical bone, located on the outside, is hard and dense, and its thickness varies according to the mechanical

stress; at the opposite extreme is cancellous or trabecular bone, which is generally located on the inside of the bones and is characterized by being light and having a trabecular lattice shape, with sufficient space to accommodate the marrow [36][37][38]. The great acceptance of synthetic HAP in implants or prostheses lies in its high crystallinity and the absence of carbonate, which leads to a much lower biodegradation compared to bone mineral nanocrystals. In addition, synthetic HAP facilitates the formation of chemical bonds with the host bone [39]. On the other hand, porosity control is crucial, as it provides a surface chemistry that allows bone tissue ingrowth, improving the mechanical attachment of the implant to the implantation site; in fact, if an implanted porous ceramic is progressively replaced by natural bone, its biomechanical properties become more and more similar to natural bone tissue. The importance of porosity in HAP implants has been previously documented. Minimal pore size and connectivity is required for the growth of blood vessels within the implant, a phenomenon known as osteoconduction [40][41][42][43]. Size is one of the most critical characteristics of the pores, since: pores smaller than 10 μm prevent cell access; pores from 10 to 50 μm allow penetration of fibrovascular tissue; from 50 to 150 μm allow bone penetration; pores larger than 150 μm allow bone penetration and formation [44][45]. Additionally, bone tissue penetration has been found to be possible only if pores are interconnected, but not in those that end blind [46]. Early studies conducted by Korkusov et al. [47] demonstrated that porous HAP implants are not only biomechanically stable, but in addition, there are no differences between the implanted and adjacent bone, an increase in osteoblastic activity and the stiffness in bending increased during bone healing was noted. Several authors stressed that the origin of the bioactivity of the HAP lies in the affinity of the hydroxyl groups of HAP for the amino acids, proteins and organic acids in the human body via hydrogen bonding [48]. One of the first papers documenting multistage pore formation appears in 1995, here the authors present to us the synthesis of HAP tapes made from dibasic calcium phosphate and calcium carbonate. On the basis of their experimental evidence, they conclude that the transformation of the starting powders into stoichiometric HAP occurs in two stages. The first, at about 45 °C characterized by a loss of water vapor from the calcium phosphate and a collapse of the original porosity. The second stage, at around 800 °C, involves further water loss and carbon dioxide evolution. The latter is associated with the decomposition of the calcium carbonate particles, being the responsibility of the final porous structure [49]. Klein et al. [50] succeeded in forming HAP cylinders of diameter 3.5 mm and length 7 mm, with a pore size distribution between 75 and 550 μm and between 45 and 60% porosity. Foaming methods were also employed for the synthesis of macropores in HAP structures and obtained very good pore interconnection and high porosity (60–90%) [51].

3. Particular Routes of Hydroxyapatite Synthesis

The idea of this subsection is to expose different alternative routes, which, although they do not have the impact of the three major routes already exposed, offer interesting opportunities that could have relevance in the immediate future. For example, biomimetic synthesis approaches can offer several advantages over conventional inorganic synthesis routes. In this sense, both new technologies and original and audacious approaches offer multiple advantages at the environmental level, in the pursuit of specific objectives or as contributions aimed at economizing certain process parameters (time, resources, energy, pollution, etc.). On the other hand, the

enormous amount of organic waste generated by the food industry can offer a very interesting source of raw material.

Milovac et al. [52] transformed natural aragonite from cuttlefish bone into HAP by a simple method based on hydrothermal transformation at 200 °C. The resulting product retained the cuttlebone architecture preserving the natural well interconnected channeled structure, Figure 2. This scaffold is suitable for cell attachment, proliferation and differentiation. A mechanochemical process (ball milling and heat treatment at 1000 °C) was applied to a mixture of recycled seashell and phosphoric acid to obtain high crystallinity and bioactive HAP [53]. Hen's eggshell was the raw material to get powder-like single phase HAP in the form of globules from 4 to 5 mm, thermally stable up to 900 °C. SEM data demonstrated that the globules consist of particles with an average size of about 30 nm [54]. The same source, eggshell, was also successfully used to synthesize a porous nanohydroxyapatite/collagen composite scaffold similar to the extracellular matrices of bone and cartilage tissues. For this purpose, HAP was nucleated in the collagen matrix. The final size of the HAP was 10 nm, polycrystalline in nature and perfectly integrated into the scaffold. The scaffold showed high porosity (95–98%) with high interconnection. In addition, the mechanical strength of the scaffold doubled with the incorporation of HAP [55]. Smooth egg-shell membranes were used as a support for the formation of hydroxyapatite agglomerates in the form of a flower. The study, experimental and theoretical, shows the driving force of ions, the effect of temperature, pH and time on the morphology and crystallinity of the aggregates. These results provide important insights into the process of bone formation [56]. A combination of natural bone and shrimp shell was employed as a scaffold to be magnetically doped with Fe3O4 and Fe2O3 nanoparticle. Although the presence of the nanoparticles reduced the porosity of the matrix, the composite showed a magnetization of 3.04 emu/g [57]. Bovine cortical bone was used after heat treatment in air at 800 °C and milling to obtain HAP, then, proportional amounts of HAP and magnetic nanoparticles (Fe3O4) were compressed at 50 MPa to create the pellets. The presence of the magnetic nanoparticles in the scaffolds enhanced cell proliferation compared to pure hydroxyapatite scaffolds [58]. Ding et al. reported a facile microwave-assisted hydrothermal preparation of amorphous calcium phosphate porous hollow microspheres using adenosine triphosphate disodium salt (Na2ATP), CaCl2 and soybean lecithin in aqueous solution. This route allows modifying morphology and structure by adjusting temperature and concentrations. The hollow microspheres are suitable for drug delivery purposes [59]. Pectin, obtained from the peel of prickly pear was used as scaffold to produce, in a simple and green method, uniform HAP nanoparticles of around 25 nm. with improved antimicrobial activity towards the test pathogenic S. aureus, E. coli bacterial strains and C. albicans [60]. Interesting work, aimed at understanding the effect of amino acids on bone formation, was carried out by Wang et al. [61]. The authors use glutamic acid and phosphoserine to modify the structure of HAP nanocrystals. The crystals obtained without amino acids were needle-like, while crystals synthesized in the presence of the amino acids presented a platy morphology with a preferred crystal orientation on (300) face, indicating preferential adsorption and suppression of growth in specific crystal directions. The adsorption of the amino acids on the HAP surface was analyzed by molecular dynamic simulations and the results exposed that amino acids may act as effective regulators in bone biomineralization. In this same line, the dual role of acidic amino acids from non-collagenous proteins was also demonstrated [62]. The amount and place of absorption of the amino acid on the materials surface rules the aggregation evens by promoting HAP crystallization at high concentrations and inhibiting it at low concentrations.

In addition, they can also change the morphology of the material by creating chain-like (Figure 3a) or liquid-like aggregates (Figure 3b).

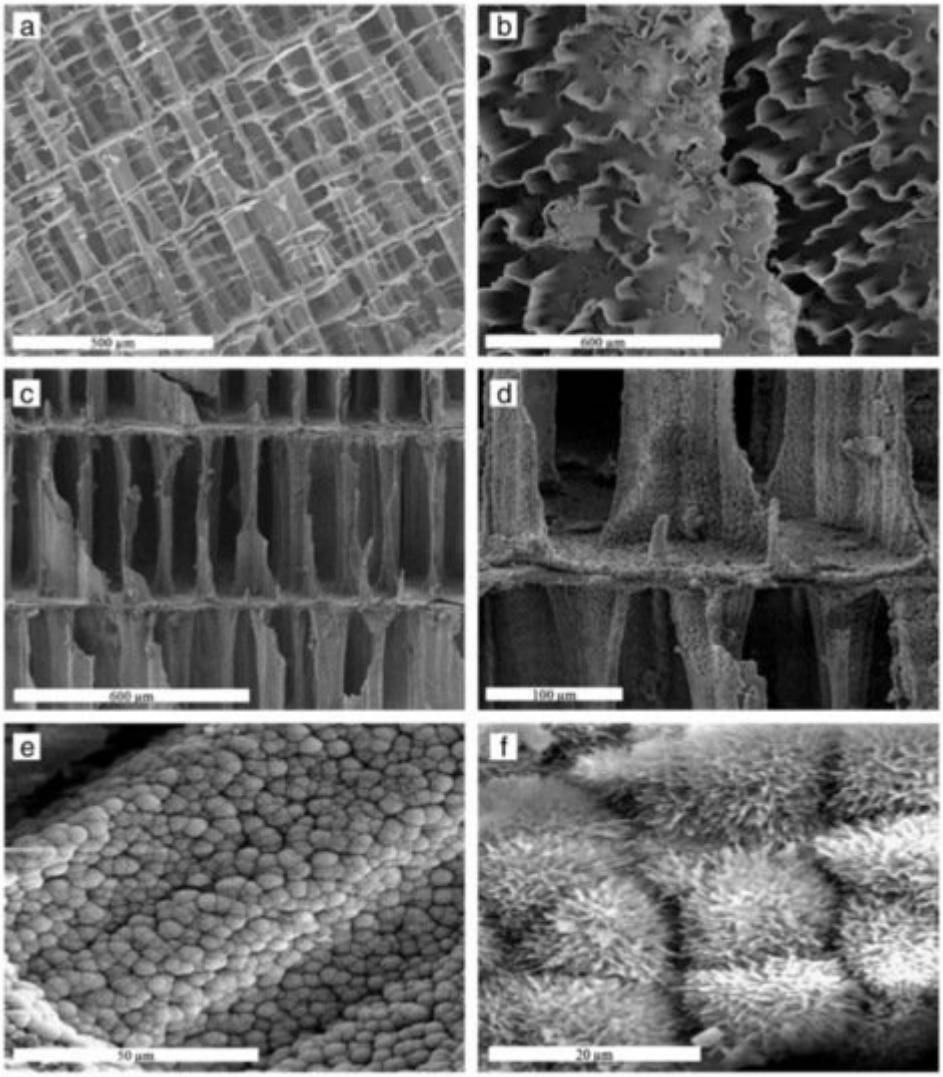

Figure 2. SEM images of cuttlefish bone (**a**,**b**) and cuttlefish bone after transformation into HAP (**c**–**f**). (**a**) Transverse cross-section (**b**) Pores formed by convoluted pillar (**c**,**d**) Transverse cross-section showing interconnected pores after transformation, (**e**) Aggregates of HAP and (**f**) dandelion-like structures. With permission from Elsevier https://doi.org/10.1016/j.msec.2013.09.036 (accessed on 19 May 2021).

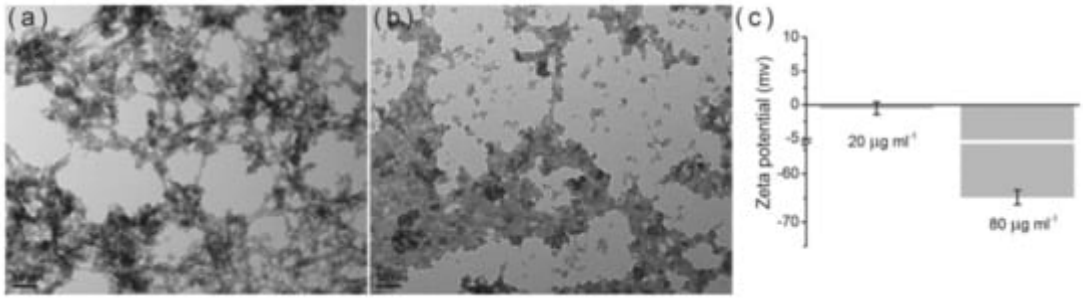

Figure 3. Effect of amino acid concentration on HAP particles: (**a**) low concentration; (**b**) high concentration. (**c**) zeta potential of the nanoparticles. With permission from Elsevier. https://doi.org/10.1016/j.jcrysgro.2020.125991 (accessed on 1 March 2021).

Hutchens et al. [56] demonstrated that bacterial cellulose provides a template for the formation of biocompatible HAP spherical clusters, formed from an octacalcium phosphate precursor similar to physiological bone, with anisotropic 10–50 nm crystals elongated in the c-axis mimicking the geometry of bone apatite crystals. Different bile salts mixed aggregates were used as templates of spongy-silica materials in an approach to simulate the trabecular bone organization, from which under specific conditions the resulting materials showed an open bioactive macropore structure [63]. Nie et al. incorporated HAP into a poly(lactic-co-glycolic acid) (PLGA) matrix to prepare HAP/PLGA composites with improved cell adhesion on the composites [64]. Cui et al. prepared (polyD,L-lactic acid) PDLLA/HAP composites through the in situ growth of HAP in PDLLA, and a stable interfacial bonding was formed between them, leading to an improved tensile strength and Young's modulus [65]. Additive manufacturing techniques provide flexible and precise controls over the size and complex shape through a layer-by-layer process but the density and mechanical properties with the printed base materials are often rare. In a recent study, the authors were able to remedy this shortcoming by using digital light processing three dimensional printing technology with mechanical results very close to the best obtained from conventional ceramic processing and sintering [66].

Li et al. [67] developed a method to construct porous hydroxyapatite by dual-phase mixing, in which the porous ceramic body and the pore-forming template are generated simultaneously. For this, the authors used a mixture of two immiscible phases: HAP slurry and polymethylmethacrylate resin. The mixture obtained is molded and subjected to polymerization, drying, pyrolysis and sintering. By controlling parameters such as viscosity, concentration ratio or mixing time and speed, it is possible to adjust porosity, pore size and interconnectivity. The material obtained was tested and proved to be sufficiently resistant for cell culture and implant handling.

Most of the production processes for 3D scaffolds are based on high temperature sintering of HAP nanoparticles for several hours. However, these processes can modify the physicochemical and biological properties of the nanoparticles, losing similarity to bone tissue. To avoid these alterations, an alternative process has been proposed in which a sodium silicate solution is used as a mineral binder for the sinterization of HAP nanoparticles by a dehydration-drying process at a low temperature (37 °C). The analysis of the final product demonstrated the viability of the new route, since from a nanoscale point of view it preserves the low crystallinity, Ca/P ratio and original size of the nanoparticles, key aspects in materials for bone regeneration. Moreover, from the microscale, the 3D scaffold has an adequate porosity and mechanical profile [68]. Silicon was also an important component of the comprehensive and rigorous study on the effect of type and chemistry of the fuel in the solution combustion synthesis process on the final properties of silicon-doped calcium phosphates carried by Farzad et al. [69]. The use of glycine as a fuel results in a higher enthalpy of combustion and concentration of gaseous by-products. The silicon-doped samples showed cytocompatibility and osteogenic potential. While the glycine and silicon mixture showed the best biological performance and the best structural and physicochemical properties.

Cyclohexane, and mixed poly (oxyethylene), nonylphenol ether were the three basic components used by Lim and his collaborators [70] in a now classic work to form a stable microemulsion to produce hydroxyapatite particles with a higher sintered density and that are more refined in grain size than that of the emulsion-derived synthesis. By optimizing the values of calcination temperature, pH and amount of components, several authors obtained a substantial improvement of the traditional Rathje method [71]. Thanks to this progress, a complete dissociation of the precursors and a refined microstructure were achieved, confirming the possibility of extending the natural precursors range for HAP preparation in an ecofriendly and cost-efficient source for bioceramics for medical applications [72]. The cytocompatibility, osteoconductivity and osteoinductivity of the materials obtained by this new route was also evaluated by the authors, although in a different article [73].

In a recent work the effect of different matrix components on the steps and processes taking place in the formation of HAP from an amorphous calcium phosphate (ACP) precursor phase was investigated. In the absence of additives, the process starts with the formation of ion pairs that subsequently lead to the appearance of an ACP phase that in the last step is transformed into HAP. In the presence of alginate-based additives, the formation and lifetime of the ACP phase can be modified due to the stabilization of the intermediate pairs. In the presence of guluronate-unit (G-unit) additives, the final precipitates were composed of a mixture of octacalcium phosphate and HAP. The work helps to understand the complex biomineralization processes in the presence of multiple components [74]. Sans et al. [75] developed a robust method based on hydrothermal methods but without using any additive, only using organic solvent to produces pure and crystalline HAP with a controlled shape and size. Here, ethanol has been proven to allow the control of the crystals' morphology (spherical polymorphs, rods, and belts, see Figure 4) through pH and their sizes through ion concentration. The formation of needle flake-like crystals and micrometric rods was achieved with different solvents and pH.

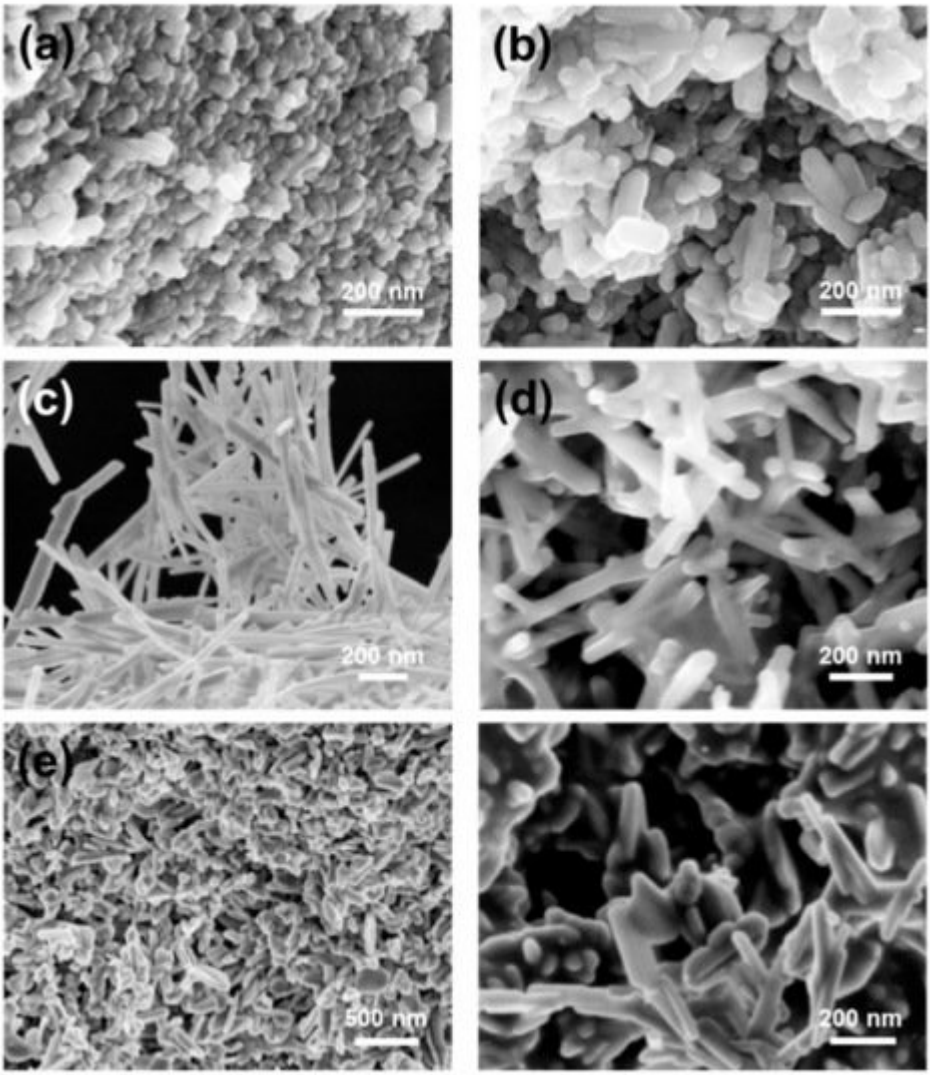

Figure 4. Different morphologies of HAP obtained from the methods proposed by Sans et al. [75]: (**a**) spherical polymorphs; (**b**) rod shapes; (**c**) belts; (**d**) belts with smaller aspect ratio; (**e**) low magnification of needle-flakes; and high magnification of needle-flakes. With permission from ACS Publications. https://doi.org/10.1021/acs.cgd.0c00850 (accessed on 5 April 2021).

References

1. Hecht, E. An historico-critical account of potential energy: Is PE really real? Phys. Teach. 2003, 41, 486–493.
2. Fratzl, P. Biomimetic materials research: What can we really learn from nature's structural materials? J. R. Soc. Interface 2007, 4, 637–642.
3. McShea, D.W. The hierarchical structure of organisms: A scale and documentation of a trend in the maximum. Paleobiology 2001, 27, 405–423.

4. Vallet-Regi, M. Bio-Ceramics with Clinical Applications; John Wiley & Sons: Hoboken, NJ, USA, 2014.
5. Colilla, M.; Manzano, M.; Vallet-Regí, M. Recent advances in ceramic implants as drug delivery systems for biomedical applications. Int. J. Nanomed. 2008, 3, 403–414.
6. Hidouri, M.; Dorozhkin, S.V.; Albeladi, N. Thermal behavior, sintering and mechanical characterization of multiple ion-substituted hydroxyapatite bioceramics. J. Inorg. Organomet. Polym. Mater. 2019, 29, 87–100.
7. Larsen, P.; Von Ins, M. The rate of growth in scientific publication and the decline in coverage provided by Science Citation Index. Scientometrics 2010, 84, 575–603.
8. Boom time for biomaterials. Nat. Mater. 2009, 8, 439.
9. Ripamonti, U. Osteoinduction in porous hydroxyapatite implanted in heterotopic sites of different animal models. Biomaterials 1996, 17, 31–35.
10. Mohammadi, Z.; Dummer, P.M.H. Properties and applications of calcium hydroxide in endodontics and dental traumatology. Int. Endod. J. 2011, 44, 697–730.
11. Meleshko, A.A.; Tolstoy, V.P.; Afinogenov, G.E.; Levshakova, A.S.; Afinogenova, A.G.; Muldiyarov, V.P.; Vissarionov, S.V.; Linnik, S.A. Prospects of hydroxyapatite-based nanomaterials application synthesized by layer-by-layer method for pediatric traumatology and orthopedics. Probl. Endocrinol. 2020, 8, 217–230.
12. Sobti, M.M.; Shams, F.; Jawaheer, L.; Cauchi, P.; Chadha, V. Unwrapped hydroxyapatite orbital implants: Our experience in 347 cases. Eye 2020, 34, 675–682.
13. Prakasam, M.; Locs, J.; Salma-Ancane, K.; Loca, D.; Largeteau, A.; Berzina-Cimdina, L. Fabrication, Properties and Applications of Dense Hydroxyapatite: A Review. J. Funct. Biomater. 2015, 6, 1099–1140.
14. Liu, Y.; Wang, W.; Zhan, Y.; Zheng, C.; Wang, G. A simple route to hydroxyapatite nanofibers. Mater. Lett. 2002, 56, 496–501.
15. Zhang, Q.-Q.; Zhu, Y.-J.; Wu, J.; Shao, Y.-T.; Cai, A.-Y.; Dong, L.-Y. Ultralong Hydroxyapatite Nanowire-Based Filter Paper for High-Performance Water Purification. ACS Appl. Mater. Interfaces 2019, 11, 4288–4301.
16. Orlovskii, V.; Komlev, V.; Barinov, S. Hydroxyapatite and hydroxyapatite-based ceramics. Inorg. Mater. 2002, 38, 973–984.
17. Zhao, Z.; Espanol, M.; Guillem-Marti, J.; Kempf, D.; Diez-Escudero, A.; Ginebra, M.-P. Ion-doping as a strategy to modulate hydroxyapatite nanoparticle internalization. Nanoscale 2016, 8, 1595–1607.

18. Zeitz, C.; Faidt, T.; Grandthyll, S.; Hähl, H.; Thewes, N.; Spengler, C.; Schmauch, J.R.; Deckarm, M.J.; Gachot, C.; Natter, H. Synthesis of hydroxyapatite substrates: Bridging the gap between model surfaces and enamel. ACS Appl. Mater. Interfaces 2016, 8, 25848–25855.
19. Ramesh, S.; Tan, C.; Tolouei, R.; Amiriyan, M.; Purbolaksono, J.; Sopyan, I.; Teng, W. Sintering behavior of hydroxyapatite prepared from different routes. Mater. Des. 2012, 34, 148–154.
20. Liu, D.-M.; Troczynski, T.; Tseng, W.J. Water-based sol–gel synthesis of hydroxyapatite: Process development. Biomaterials 2001, 22, 1721–1730.
21. Mahabole, M.; Aiyer, R.; Ramakrishna, C.; Sreedhar, B.; Khairnar, R. Synthesis, characterization and gas sensing property of hydroxyapatite ceramic. Bull. Mater. Sci. 2005, 28, 535–545.
22. Pu'ad, N.M.; Haq, R.A.; Noh, H.M.; Abdullah, H.; Idris, M.; Lee, T. Synthesis method of hydroxyapatite: A review. Mater. Today Proc. 2020, 29, 233–239.
23. Cox, S.C.; Walton, R.I.; Mallick, K.K. Comparison of techniques for the synthesis of hydroxyapatite. Bioinspired Biomim. Nanobiomater. 2015, 4, 37–47.
24. Rhee, S.-H. Synthesis of hydroxyapatite via mechanochemical treatment. Biomaterials 2002, 23, 1147–1152.
25. Yeong, K.; Wang, J.; Ng, S. Mechanochemical synthesis of nanocrystalline hydroxyapatite from CaO and CaHPO4. Biomaterials 2001, 22, 2705–2712.
26. Liu, D.-M.; Yang, Q.; Troczynski, T.; Tseng, W.J. Structural evolution of sol–gel-derived hydroxyapatite. Biomaterials 2002, 23, 1679–1687.
27. Hsieh, M.-F.; Chin, T.-S.; Perng, L.-H.; Perng, H.-G. Gel-to-Ceramic Conversion during Hydroxyapatite Synthesis. J. Am. Ceram. Soc. 2001, 84, 2123–2125.
28. Seckler, M.; Danese, M.; Derenzo, S.; Valarelli, J.; Giulietti, M.; Rodríguez-Clemente, R. Influence of process conditions on hydroxyapatite crystallinity obtained by direct crystallization. Mater. Res. 1999, 2, 59–62.
29. Weng, W.; Baptista, J. A new synthesis of hydroxyapatite. J. Eur. Ceram. Soc. 1997, 17, 1151–1156.
30. Velayudhan, S.; Ramesh, P.; Sunny, M.; Varma, H. Extrusion of hydroxyapatite to clinically significant shapes. Mater. Lett. 2000, 46, 142–146.
31. Rodríguez-Lugo, V.; Karthik, T.; Mendoza-Anaya, D.; Rubio-Rosas, E.; Villaseñor Cerón, L.; Reyes-Valderrama, M.; Salinas-Rodríguez, E. Wet chemical synthesis of nanocrystalline hydroxyapatite flakes: Effect of pH and sintering temperature on structural and morphological properties. R. Soc. Open Sci. 2018, 5, 180962.

32. Yelten-Yilmaz, A.; Yilmaz, S. Wet chemical precipitation synthesis of hydroxyapatite (HA) powders. Ceram. Int. 2018, 44, 9703–9710.
33. Ramesh, S.; Adzila, S.; Tan, C. Properties of hydroxyapatite synthesize by wet chemical method. J. Ceram. Process. Res. 2013, 14, 448–452.
34. Chen, F.; Zhu, Y.-J. Large-Scale Automated Production of Highly Ordered Ultralong Hydroxyapatite Nanowires and Construction of Various Fire-Resistant Flexible Ordered Architectures. ACS Nano 2016, 10, 11483–11495.
35. Gomes, D.; Santos, A.; Neves, G.; Menezes, R. A brief review on hydroxyapatite production and use in biomedicine. Cerâmica 2019, 65, 282–302.
36. Majumdar, S.; Genant, H.; Grampp, S.; Newitt, D.; Truong, V.H.; Lin, J.; Mathur, A. Correlation of trabecular bone structure with age, bone mineral density, and osteoporotic status: In vivo studies in the distal radius using high resolution magnetic resonance imaging. J. Bone Mineral. Res. 1997, 12, 111–118.
37. Vogler, J., 3rd; Murphy, W. Bone marrow imaging. Radiology 1988, 168, 679–693.
38. Olszta, M.J.; Cheng, X.; Jee, S.S.; Kumar, R.; Kim, Y.-Y.; Kaufman, M.J.; Douglas, E.P.; Gower, L.B. Bone structure and formation: A new perspective. Mater. Sci. Eng. R Rep. 2007, 58, 77–116.
39. Tadic, D.; Beckmann, F.; Schwarz, K.; Epple, M. A novel method to produce hydroxyapatite objects with interconnecting porosity that avoids sintering. Biomaterials 2004, 25, 3335–3340.
40. Yoshikawa, H.; Myoui, A. Bone tissue engineering with porous hydroxyapatite ceramics. J. Artif. Organs 2005, 8, 131–136.
41. Sopyan, I.; Mel, M.; Ramesh, S.; Khalid, K. Porous hydroxyapatite for artificial bone applications. Sci. Technol. Adv. Mater. 2007, 8, 116.
42. Nie, W.; Peng, C.; Zhou, X.; Chen, L.; Wang, W.; Zhang, Y.; Ma, P.X.; He, C. Three-dimensional porous scaffold by self-assembly of reduced graphene oxide and nano-hydroxyapatite composites for bone tissue engineering. Carbon 2017, 116, 325–337.
43. Türk, S.; Altınsoy, I.; Efe, G.Ç.; İpek, M.; Özacar, M.; Bindal, C. 3D porous collagen/functionalized multiwalled carbon nanotube/chitosan/hydroxyapatite composite scaffolds for bone tissue engineering. Mater. Sci. Eng. C 2018, 92, 757–768.
44. Le Huec, J.; Schaeverbeke, T.; Clement, D.; Faber, J.; Le Rebeller, A. Influence of porosity on the mechanical resistance of hydroxyapatite ceramics under compressive stress. Biomaterials 1995, 16, 113–118.
45. Chang, B.-S.; Hong, K.-S.; Youn, H.-J.; Ryu, H.-S.; Chung, S.-S.; Park, K.-W. Osteoconduction at porous hydroxyapatite with various pore configurations. Biomaterials 2000, 21, 1291–1298.

46. Itoh, S.; Nakamura, S.; Nakamura, M.; Shinomiya, K.; Yamashita, K. Enhanced bone ingrowth into hydroxyapatite with interconnected pores by Electrical Polarization. Biomaterials 2006, 27, 5572–5579.
47. Korkusuz, F.; Karamete, K.; Irfanoğlu, B.; Yetkin, H.; Hastings, G.W.; Akkas, N. Do porous calcium hydroxyapatite ceramics cause porosis in bone? A bone densitometry and biomechanical study on cortical bones of rabbits. Biomaterials 1995, 16, 537–543.
48. Gao, C.; Peng, S.; Feng, P.; Shuai, C. Bone biomaterials and interactions with stem cells. Bone Res. 2017, 5, 17059.
49. Arita, I.H.; Wilkinson, D.S.; Mondragón, M.A.; Castaño, V.M. Chemistry and sintering behaviour of thin hydroxyapatite ceramics with controlled porosity. Biomaterials 1995, 16, 403–408.
50. Klein, C.; de Groot, K.; Chen, W.; Li, Y.; Zhang, X. Osseous substance formation induced in porous calcium phosphate ceramics in soft tissues. Biomaterials 1994, 15, 31–34.
51. Ozgür Engin, N.; Tas, A.C. Manufacture of macroporous calcium hydroxyapatite bioceramics. J. Eur. Ceram. Soc. 1999, 19, 2569–2572.
52. Milovac, D.; Gallego Ferrer, G.; Ivankovic, M.; Ivankovic, H. PCL-coated hydroxyapatite scaffold derived from cuttlefish bone: Morphology, mechanical properties and bioactivity. Mater. Sci. Eng. C 2014, 34, 437–445.
53. Pal, A.; Maity, S.; Chabri, S.; Bera, S.; Chowdhury, A.R.; Das, M.; Sinha, A. Mechanochemical synthesis of nanocrystalline hydroxyapatite from Mercenaria clam shells and phosphoric acid. Biomed. Phys. Eng. Express 2017, 3, 015010.
54. Goloshchapov, D.L.; Kashkarov, V.M.; Rumyantseva, N.A.; Seredin, P.V.; Lenshin, A.S.; Agapov, B.L.; Domashevskaya, E.P. Synthesis of nanocrystalline hydroxyapatite by precipitation using hen’s eggshell. Ceram. Int. 2013, 39, 4539–4549.
55. Padmanabhan, S.K.; Salvatore, L.; Gervaso, F.; Catalano, M.; Taurino, A.; Sannino, A.; Licciulli, A. Synthesis and characterization of collagen scaffolds reinforced by eggshell derived hydroxyapatite for tissue engineering. J. Nanosci. Nanotechnol. 2015, 15, 504–509.
56. Zhang, Y.; Liu, Y.; Ji, X.; Banks, C.E.; Song, J. Flower-like agglomerates of hydroxyapatite crystals formed on an egg-shell membrane. Colloids Surf. B Biointerfaces 2011, 82, 490–496.
57. Heidari, F.; Bahrololoom, M.E.; Vashaee, D.; Tayebi, L. In situ preparation of iron oxide nanoparticles in natural hydroxyapatite/chitosan matrix for bone tissue engineering application. Ceram. Int. 2015, 41, 3094–3100.
58. Maleki-Ghaleh, H.; Aghaie, E.; Nadernezhad, A.; Zargarzadeh, M.; Khakzad, A.; Shakeri, M.; Khosrowshahi, Y.B.; Siadati, M. Influence of Fe3O4 nanoparticles in hydroxyapatite scaffolds on proliferation of primary human fibroblast cells. J. Mater. Eng. Perform. 2016, 25, 2331–2339.

59. Ding, G.-J.; Zhu, Y.-J.; Qi, C.; Lu, B.-Q.; Chen, F.; Wu, J. Porous hollow microspheres of amorphous calcium phosphate: Soybean lecithin templated microwave-assisted hydrothermal synthesis and application in drug delivery. J. Mater. Chem. B 2015, 3, 1823–1830.
60. Gopi, D.; Kanimozhi, K.; Kavitha, L. Opuntia ficus indica peel derived pectin mediated hydroxyapatite nanoparticles: Synthesis, spectral characterization, biological and antimicrobial activities. Spectrochim. Acta Part A Mol. Biomol. Spectrosc. 2015, 141, 135–143.
61. Wang, Z.; Xu, Z.; Zhao, W.; Sahai, N. A potential mechanism for amino acid-controlled crystal growth of hydroxyapatite. J. Mater. Chem. B 2015, 3, 9157–9167.
62. Jiang, S.; Cao, Y.; Li, S.; Pang, Y.; Sun, Z. Dual function of poly(acrylic acid) on controlling amorphous mediated hydroxyapatite crystallization. J. Cryst. Growth 2021, 557, 125991.
63. Fernández-Leyes, M.; Verdinelli, V.; Hassan, N.; Ruso, J.M.; Pieroni, O.; Schulz, P.C.; Messina, P. Biomimetic formation of crystalline bone-like apatite layers on spongy materials templated by bile salts aggregates. J. Mater. Sci. 2012, 47, 2837–2844.
64. Nie, H.; Wang, C.-H. Fabrication and characterization of PLGA/HAp composite scaffolds for delivery of BMP-2 plasmid DNA. J. Control. Release 2007, 120, 111–121.
65. Cui, W.; Li, X.; Chen, J.; Zhou, S.; Weng, J. In Situ Growth Kinetics of Hydroxyapatite on Electrospun Poly(dl-lactide) Fibers with Gelatin Grafted. Cryst. Growth Des. 2008, 8, 4576–4582.
66. Yao, Y.; Qin, W.; Xing, B.; Sha, N.; Jiao, T.; Zhao, Z. High performance hydroxyapatite ceramics and a triply periodic minimum surface structure fabricated by digital light processing 3D printing. J. Adv. Ceram. 2021, 10, 39–48.
67. Li, S.H.; de Wijn, J.R.; Layrolle, P.; de Groot, K. Novel method to manufacture porous hydroxyapatite by dual-phase mixing. J. Am. Ceram. Soc. 2003, 86, 65–72.
68. Lakrat, M.; Jabri, M.; Alves, M.; Fernandes, M.H.; Ansari, L.L.; Santos, C.; Mejdoubi, E.M. Three-dimensional nano-hydroxyapatite sodium silicate glass composite scaffold for bone tissue engineering-A new fabrication process at a near-room temperature. Mater. Chem. Phys. 2021, 260, 124185.
69. Kermani, F.; Gharavian, A.; Mollazadeh, S.; Kargozar, S.; Youssefi, A.; Khaki, J.V. Silicon-doped calcium phosphates; the critical effect of synthesis routes on the biological performance. Mater. Sci. Eng. C 2020, 111, 110828.
70. Lim, G.; Wang, J.; Ng, S.; Chew, C.; Gan, L. Processing of hydroxyapatite via microemulsion and emulsion routes. Biomaterials 1997, 18, 1433–1439.
71. Rathje, W. Zur Kenntnis der Phosphate I: Über Hydroxylapatit. Bodenkd. Pflanz. 1939, 12, 121–128.

72. Miculescu, F.; Mocanu, A.-C.; Dascălu, C.A.; Maidaniuc, A.; Batalu, D.; Berbecaru, A.; Voicu, S.I.; Miculescu, M.; Thakur, V.K.; Ciocan, L.T. Facile synthesis and characterization of hydroxyapatite particles for high value nanocomposites and biomaterials. Vacuum 2017, 146, 614–622.
73. Mitran, V.; Ion, R.; Miculescu, F.; Necula, M.G.; Mocanu, A.-C.; Stan, G.E.; Antoniac, I.V.; Cimpean, A. Osteoblast Cell Response to Naturally Derived Calcium Phosphate-Based Materials. Materials 2018, 11, 1097.
74. Ucar, S.; Bjørnøy, S.H.; Bassett, D.C.; Strand, B.L.; Sikorski, P.; Andreassen, J.-P. Formation of hydroxyapatite via transformation of amorphous calcium phosphate in the presence of alginate additives. Cryst. Growth Des. 2019, 19, 7077–7087.
75. Sans, J.; Sanz, V.; Puiggalí, J.; Turon, P.; Alemán, C. Controlled Anisotropic Growth of Hydroxyapatite by Additive-Free Hydrothermal Synthesis. Cryst. Growth Des. 2020, 2, 748–756.